Kinematic analysis of the 3-PRPR redundant planar parallel manipulator

M. Ruggiu[1], J. A. Carretero[2]

[1] *Dept. of Mechanical Engineering, University of Cagliari, Cagliari, Italy, e-mail: ruggiu@dimeca.unica.it*

[2] *Dept. of Mechanical Eng., University of New Brunswick, Fredericton, NB, Canada, e-mail: Juan.Carretero@unb.ca*

Abstract

In this paper the 3-PRPR redundant planar parallel manipulator is introduced and thoroughly analysed. The analysis consists on: a) the solution of the forward (direct) displacement problem using an analytical procedure; b) the geometrical determination of the orientational workspace; c) the solution of the inverse displacement problem; d) the solution of the forward velocity problem; and finally, e) the determination of the direct and inverse singularities by inspecting the manipulator's Jacobian matrices. The singularity analysis includes the geometrical interpretation of the singularity conditions. It was found that the direct singularities are equivalent to those of the typical non-redundant 3-RRR manipulator. Conversely, the inverse singularities may only occur when the displacement of one or more of the prismatic joints is equal to zero which, in a typical implementation this would not be possible.

Keywords: planar parallel manipulator, kinematic redundancy, forward kinematics, inverse kinematics, singularities.

Analyse cinématique du manipulateur redondant plan de type 3-PRPR

Résumé

Cet article introduit un nouveau manipulateur redondant parallèle plan. Le manipulateur qui a une architecture symétrique de type 3-PRPR, est analysé en détail. L'analyse cinématique comprends : a) la solution du problème géométrique direct ; b) la détermination par méthode géométrique de l'espace de travail du manipulateur ; c) la solution du problème géométrique inverse ; d) la solution de la cinématique directe ; et enfin, e) la détermination des singularités directes et inverses à travers de l'inspection des matrices jacobiennes. L'analyse des singularités inclut l'interprétation géométrique des conditions qui produisent les singularités. Les résultats de l'analyse montrent que les singularités directes sont équivalents à ceux du manipulateur non redondant de type 3-RRR. Par contre, les singularités inverses existent seulement quand un ou plus des actionneurs prismatiques ont une valeur de zéro ce qui est peu probable dans une implémentions réelle.

Mots-clé: manipulateur parallèle plan, redondance cinématique, cinématique directe, cinématique inverse, singularitées.

---

1 INTRODUCTION

In the last few decades, parallel manipulators have attracted significant attention from the robotics community. The main reasons for this are their well accepted advantages in comparison to the serial ones such as: high structural rigidity, high payload-to-weight ratio and relatively high accuracy, amongst other. However, they have a number of drawbacks: complexity in their forward kinematic equations, relatively small workspace, singularities inside the workspace, to name a few. Some of the cited drawbacks, namely the singularities inside their workspace and a generally small workspace, may be overcome by the use of redundancy. In parallel manipulators, there are three basic types of redundancy:

a) *Kinematic redundancy* consists of adding extra active joints and links to one or more branches of the mechanism [1, 2, 3]. In this case the added mobility of the mechanism allows for an enlarged workspace while helping avoid most singular configurations [4, 5].

b) *Actuation redundancy* consists of replacing passive joints by active ones. In doing so, the number of DOF (degrees-of-freedom) of the manipulator does not change. Actuation redundancy reduces or eliminates certain types of singular configurations within the manipulator's workspace [6, 7].

c) *Branch redundancy* refers to the addition of extra actuated branches to the manipulator [8]. Branch redundancy normally allows for improved force capabilities and reduction of most singular configurations.

Despite the cited advantages of redundant parallel manipulators over their non-redundant counterparts, they all have increased complexity of the mechanism in terms of structural design, kinematic analysis and control. For instance, in the case of *actuation or branch redundant manipulators*, an infinite number of solutions to the inverse force problem exist. That is, an infinite number of joint forces/torques combinations can produce one same force-moment couple at the end effector. As such, it is possible to have force interference which may induce harmful internal forces within the mechanism [8, 9]. This, in turn, does not allow such manipulators to be controlled using simple position control schemes [4]. Conversely, in the case of *kinematically redundant manipulators*, the focus of this paper, the inverse displacement problem (IDP) has infinite solutions for each kinematically redundant branch [2, 3]. That is, an infinite choice of joint positions and velocities exist for any particular position and velocity of the end effector. Therefore, the choice of kinematic solution (whether it is position, velocity or higher order) needs to be made using criteria such as maximise distance to singular configurations or improved dexterity [4, 5].

Ebrahimi *et al.* [3, 10] and Cha *et al.* [4] proposed a number of redundant planar parallel manipulators all with 3-$\underline{R}\underline{P}$RR, 3-$\underline{P}\underline{R}$RR, 3-RR$\underline{P}$R 3-$\underline{R}\underline{P}R\underline{P}$R architectures[3]. In this work, the 3-$\underline{P}$R$\underline{P}$R redundant planar parallel manipulator is proposed and thoroughly studied. The planar 3-$\underline{P}$R$\underline{P}$R manipulator has six actuated joints and thus has three degrees of kinematic redundancy. The motivation of this work is to analyse a manipulator with three degrees of kinematic redundancy with two active prismatic pairs per branch. The proposed architecture is the simplest of this family as the first prismatic pair is attached to the ground. The analysis that follows consists on a) solving the

[3] $\underline{P}$ and $\underline{R}$ denote actuated prismatic or revolute joints, respectively, while P and R denote passive prismatic and revolute joints, respectively.

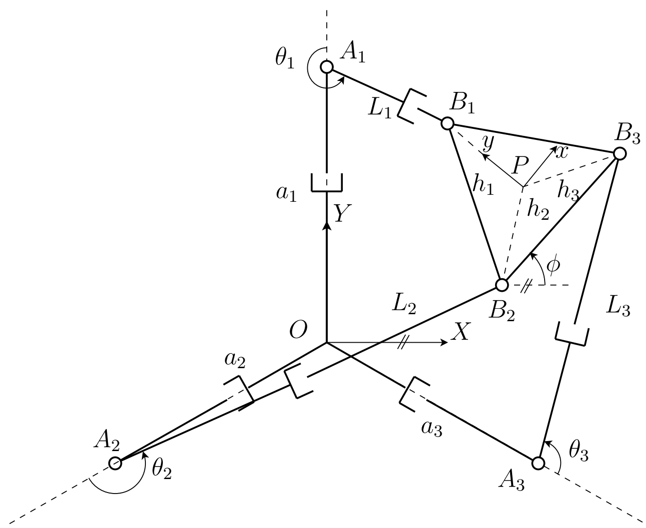

Figure 1: The 3-PRPR redundant planar parallel manipulator

forward displacement problem (FDP) using an analytical procedure, b) geometrically calculate the orientational workspace of the manipulator, c) solve the inverse displacement problem, d) solve the forward velocity problem and finally e) determine the direct and inverse singularities by inspecting the Jacobian matrices.

2 FORWARD DISPLACEMENT SOLUTION

The proposed 3-PRPR manipulator is shown in Figure 1. This kinematically redundant planar parallel manipulator consists of 3 identical legs. Each leg is a kinematic chain with a couple of PR pairs in series. The moving platform is shaped as an equilateral triangle and the prismatic pair attached to the frame are angled at $2\pi/3$ from each other with the first one aligned with the inertial Y axis. Two reference frames are defined to develop the kinematic analysis: a fixed or inertial $\{OXYZ\}$ and a frame $\{Pxyz\}$ attached to the moving platform with origin P at the centroid of the triangle and the y axis pointing in the direction of point B_1 (Figure 1).

The vector loop closure equation for each leg can be stated as:

$$\mathbf{a}_i + \mathbf{L}_i + {}^0\mathbf{R}_m {}^m\mathbf{h}_i = \mathbf{p} \tag{1}$$

where $\mathbf{a}_i = OA_i$, $\mathbf{L}_i = A_iB_i$, ${}^m\mathbf{h}_i = B_iP$, $\mathbf{p} = OP$ and ${}^0\mathbf{R}_m$ is a 3×3 proper orthonormal rotation matrix representing the orientation of the moving frame $\{Pxyz\}$ relative to the inertial frame $\{OXYZ\}$. Given that the motion of the moving platform and thus the frame $\{Pxyz\}$ is constrained on the XY plane, matrix ${}^0\mathbf{R}_m$ coincides with a basic rotation matrix expressing a rotation ϕ around the Z axis.

Note that, in equation (1), all vectors without a leading superscript are expressed in the fixed reference frame whereas vector ${}^m\mathbf{h}_i$, expressed in the moving ref. system, was multiplied by the rotation matrix ${}^0\mathbf{R}_m$ in order to express it in terms of the fixed frame.

In the forward displacement problem, the actuator variables $\mathbf{L}_i$ and $\mathbf{a}_i$ ($i = 1 \ldots 3$) are given while the elements of $\mathbf{p}$ and the angle ϕ, are solved for. To do so, equation (1) if first re-written as follows and then squared:

$$
\begin{aligned}
\mathbf{L}_i &= \mathbf{p} - \mathbf{a}_i - {}^0\mathbf{R}_m {}^m\mathbf{h}_i && (2)\\
L_i^2 &= \left(x^2+y^2\right) + a_i^2 + h_i^2 - 2\mathbf{p}\cdot\mathbf{a}_i - 2\mathbf{p}\cdot\left({}^0\mathbf{R}_m {}^m\mathbf{h}_i\right) + 2\mathbf{a}_i\cdot\left({}^0\mathbf{R}_m {}^m\mathbf{h}_i\right) && (3)
\end{aligned}
$$

where L_i, a_i and h_i are the magnitude of vectors $\mathbf{L}_i$, $\mathbf{a}_i$ and $\mathbf{h}_i$, respectively whereas x, y denote the first two Cartesian components of vector $\mathbf{p}$. The terms in the previous equations are given by:

$$
\begin{aligned}
\mathbf{a}_1 &= a_1 \left[\begin{array}{ccc} 0 & 1 & 0 \end{array}\right]^T;\\
\mathbf{a}_2 &= a_2 \left[\begin{array}{ccc} p & q & 0 \end{array}\right]^T;\\
\mathbf{a}_3 &= a_3 \left[\begin{array}{ccc} -p & q & 0 \end{array}\right]^T\\
{}^m h_1 &= h_1 \left[\begin{array}{ccc} 0 & 1 & 0 \end{array}\right]^T;\\
{}^m h_2 &= h_2 \left[\begin{array}{ccc} p & q & 0 \end{array}\right]^T;\\
{}^m h_3 &= h_3 \left[\begin{array}{ccc} -p & q & 0 \end{array}\right]^T
\end{aligned}
$$

with $p = \cos(7/6\pi)$ and $q = \sin(7/6\pi)$. Substituting the elements of these vectors into equation (3) leads to the following three equations (one for each limb):

$$
\begin{aligned}
(x - h_1 s_\phi)^2 + (y - a_1 + h_1 c_\phi)^2 - L_1^2 &= 0\\
(x - a_2 p + h_2 p c_\phi - h_2 q s_\phi)^2 + (y - a_2 q + h_2 p s_\phi + h_2 q c_\phi)^2 - L_2^2 &= 0 \qquad (4)\\
(x + a_3 p - h_3 p c_\phi - h_3 q s_\phi)^2 + (y - a_3 q - h_3 p s_\phi + h_3 q c_\phi)^2 - L_3^2 &= 0
\end{aligned}
$$

where c_* and s_* correspond to the $\cos(*)$ and $\sin(*)$, respectively.

In what follows, the half angle substitution is used to solve equations (4). First, the equations are expanded and the trigonometric identities are replaced as $c_\phi = \frac{1-t^2}{1+t^2}$, $s_\phi = \frac{2t}{1+t^2}$ with $t = \tan(\frac{\phi}{2})$. This produces a set of polynomial equations in terms of t which is then suppressed according to the Sylvester Dialytic Elimination Method. Thus, equations (4) become:

$$
\begin{aligned}
E_0 x^2 + E_1 y^2 + E_2 x + E_3 y + E_4 &= 0\\
E_0^{'} x^2 + E_1^{'} y^2 + E_2^{'} x + E_3^{'} y + E_4^{'} &= 0 \qquad (5)\\
E_0^{''} x^2 + E_1^{''} y^2 + E_2^{''} x + E_3^{''} y + E_4^{''} &= 0
\end{aligned}
$$

Explicit expressions of parameters E_k, $E_k^{'}$, $E_k^{''}$ $(k = 0 \ldots 4)$ are

$$\begin{aligned}
E_0 &= E_0^{'} = E_0^{''} = E_1 = E_1^{'} = E_1^{''} = 1 + t^2 \\
E_2 &= -4h_1 t, \\
E_2^{'} &= -2a_2 p(1+t^2) + 2ph_2(1-t^2) - 4h_2 qt, \\
E_2^{''} &= 2a_3 p(1+t^2) - 2ph_3(1-t^2) - 4h_3 qt \\
E_3 &= 2h_1(1-t^2) - 2a_1(1+t^2), \\
E_3^{'} &= -2a_2 q(1+t^2) + 2qh_2(1-t^2) + 4h_2 pt \\
E_3^{''} &= -2a_3 q(1+t^2) + 2qh_3(1-t^2) - 4h_3 pt \\
E_4 &= -2h_1 a_1(1-t^2) - D_1(1+t^2), \\
E_4^{'} &= -2h_2 a_2(1-t^2) + D_2(1+t^2), \\
E_4^{''} &= -2h_3 a_3(1-t^2) + D_3(1+t^2) \\
D_i &= a_i^2 + h_i^2 - L_i^2, \\
i &= 1, 2, 3
\end{aligned}$$

Then, the first of equations (5) is subtracted from to the other two. From which, and considering that $E_0^{'} = E_0^{''} = E_1^{'} = E_1^{''}$, the following equations are obtained:

$$E_0 x^2 + E_1 y^2 + E_2 x + E_3 y + E_4 = 0 \qquad (6)$$

$$G_1 x + G_2 y + G_3 = 0 \qquad (7)$$

$$G_4 x + G_5 y + G_6 = 0 \qquad (8)$$

where:

$$\begin{aligned}
G_1 &= E_2^{'} - E_2, G_2 = E_3^{'} - E_3, G_3 = E_4^{'} - E_4 \\
G_4 &= E_2^{''} - E_2, G_5 = E_3^{''} - E_3, G_6 = E_4^{''} - E_4
\end{aligned}$$

Equations (7) and (8) allow to obtain components x and y as follows:

$$x = H_1/H_0 \qquad (9)$$

$$y = -G_6/G_5 - G_4 x/G_5 \qquad (10)$$

with: $H_1 = (G_2G_6 - G_3G_5)/G_5$ and $H_0 = (G_1G_5 - G_4G_2)/G_5$.

Substituting equations (9) and (10) into equation (6), a polynomial equation in terms of t is obtained as:

$$\begin{aligned}
&E_0 \frac{(G_2G_6 - G_3G_5)}{(G_1G_5 - G_4G_2)^2} - E_1 \left[\frac{G_6}{G_5} + \frac{G_4}{G_5} \frac{(G_2G_6 - G_3G_5)}{(G_1G_5 - G_4G_2)^2} \right] \\
&+ E_2 \frac{(G_2G_6 - G_3G_5)}{(G_1G_5 - G_4G_2)} - E_3 \left[\frac{G_6}{G_5} + \frac{G_4}{G_5} \frac{(G_2G_6 - G_3G_5)}{(G_1G_5 - G_4G_2)} \right] + E_4 = 0 \qquad (11)
\end{aligned}$$

Equation (11) is of the sixth order. In the range -$\pi < \phi < \pi$ each solution of equation (11) provides two possible values for ϕ. However only six values of ϕ are solutions of the original system of equations (4). Therefore there are at most six solutions for the FDS of the manipulator under study.

2.1 Numerical example for the FDS

Consider the displacements values of all six actuators as given in Table 1 where l.u. denotes the length unit chosen for the calculation. The displacements were randomly selected within the actuators' imposed limits. With this data, equation (11) takes the following form:

$$2228.6t^6 - 45.76t^5 + 86.31t^4 - 47.90t^3 - 6.64t^2 - 6.85t + 1 = 0 \tag{12}$$

Solutions of equation (12) are given in Table 2. Omitting the complex solutions in Table 2, ϕ can take the values given in Table 3 whereas the corresponding coordinates of the moving platform are given in Table 4.

3 ORIENTATIONAL WORKSPACE

The orientational workspace is defined as the region where every point may be reached by a reference point on the moving platform while the platform can achieve all possible orientations (*i.e.*, any angle $-\pi < \phi < \pi$). Here, the commonly-used geometrical procedure introduced for non-redundant manipulators in [11] is used. The geometrical data used for the example presented here is given in Table 5. $h_1 = h_2 = h_3$ were chose to be equal to the unit to allow the results within this study to be easily scaled. The actuators' upper limit, *i.e.*, $a_{i_{max}}$ and $L_{i_{max}}$, were arbitrarily picked to be 5.

The orientational workspace is schematically shown in Figure 2. As it can be observed, the workspace for the symmetrical case is a circle. The radius of the circle denoting the limit of the orientational workspace is equal to $L_{i_{max}} - h_i$. The presence of two prismatic pairs provides a wide workspace. The workspace's area is about 39 times greater than the moving platform's area, in comparison with the ratio between the maximum stroke of the actuators and h_i which is only 5.

Table 6 shows the ratio R_A between the workspace and the moving platform areas, respectively A_{ws} and A_{mp} if the upper limits of the pairs or the dimension of the moving platform are changed. It is worth noting that the orientational workspace directly increase with the limit imposed on L_i (*i.e.*, $L_{i_{max}}$) while remaining invariant with respect to the limits imposed on a_i. The limits on a_i, on the other hand, influence the solution of the inverse displacement problem.

In the case of $L_{i_{max}} = 10$ [l.u.] and $h_i = 1$ [l.u.] the ratio between the workspace and the moving platform areas reaches about 196.

4 INVERSE DISPLACEMENT PROBLEM

Equations (4) may be used to solve the inverse displacement problem (IDP) as well. Since the 3-$\underline{P}R\underline{P}R$ manipulator has three degrees of kinematic redundancy, there are ∞^3 solutions of the IDP. That is, although the system of equations (4) has three independent equation, it has 6 unknowns (*i.e.*, a_i and L_i for $i = 1, 2, 3$).

For an easier physical interpretation, equations (4) can be re-written as:

Table 1: Input data for the numerical calculation of the FDS.

a_1 [l.u.]	L_1 [l.u.]	a_2 [l.u.]	L_2 [l.u.]	a_3 [l.u.]	L_3 [l.u.]
1.6	0.6	1.5	1.6	2.4	1.5

Table 2: Roots of equation (12).

t_1	t_2	t_3	t_4	t_5	t_6
0.1594	0.3023	-0.003 +0.326j	-0.2203 +0.1977j	-0.2203 -0.1977j	-0.003 -0.326j

Table 3: Values taken by ϕ (complex values are omitted).

ϕ_1	ϕ_2
0.3161	0.5871

Table 4: Coordinates of the centre of the moving platform.

$[x, y]_1^T$	$[x, y]_2^T$
$[0.8896, 0.4912]^T$	$[0.7442, 0.1984]^T$

Table 5: Geometrical data for the orientational workspace calculation.

$h_1 = h_2 = h_3$ [l.u.]	$a_{i_{min}}, a_{i_{max}}$ [l.u.]	$L_{i_{min}}, L_{i_{max}}$ [l.u.]
1	0, 5	0, 5

Table 6: Ratio A_{ws}/A_{mp} when varying a_i, L_i limits.

$h_1 = h_2 = h_3$ [l.u.]	$L_{i_{max}}$ [l.u.]	R_A
1	5	38.7
1	10	195.9
3	5	1.1
3	10	13.2

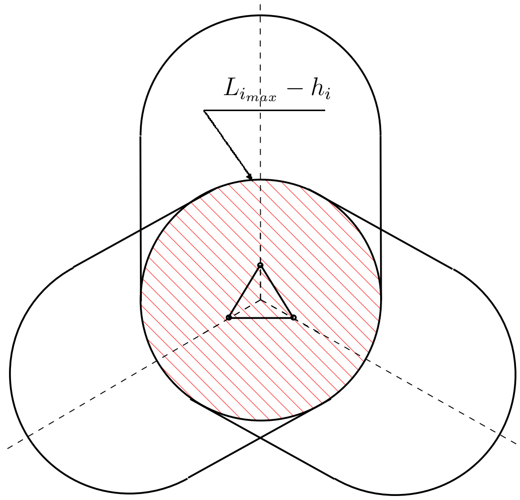

Figure 2: The orientational workspace of the symmetrical 3-PRPR manipulator.

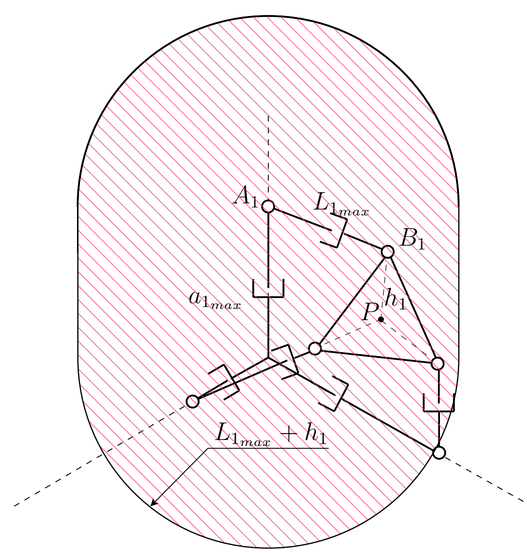

Figure 3: IDP locus solutions (branch 1)

$$
\begin{aligned}
(x_{B_1})^2 + (y_{B_1} - a_1)^2 &= L_1^2 \\
(x_{B_2} - a_2 p)^2 + (y_{B_2} - a_2 q)^2 &= L_2^2 \\
(x_{B_3} + a_3 p)^2 + (y_{B_3} - a_3 q)^2 &= L_3^2
\end{aligned} \tag{13}
$$

where x_{B_i} and y_{B_i} are the Cartesian components of the coordinates of point B_i with respect to the base frame (see Figure 1). Equations (13) represent three circles of radius L_i whose centre is positioned at a distance a_i from the origin O along the direction of the first prismatic joint on leg i. As shown in Figure 3, the locus of solutions for each leg is obtained as the envelope of a circle of radius $L_{i_{max}} + h_i$ swept along the direction of the first prismatic joint of leg i with $a_{i_{max}}$. They can be expressed as:

$$
\begin{aligned}
a_1^2 + L_1^2 - 2a_1 L_1 c_{\theta_1} = (x_{B_1} + y_{B_1})^2 \\
a_2^2 + L_2^2 - 2a_2 L_2 c_{\theta_2} = (x_{B_2} + y_{B_2})^2 \\
a_3^2 + L_3^2 - 2a_3 L_3 c_{\theta_3} = (x_{B_3} + y_{B_3})^2
\end{aligned} \tag{14}
$$

where θ_i is the angle formed by a_i and L_i directions (see Figure 1).

Thus, for a given pose of the moving platform, (*i.e.*, given x, y, ϕ and therefore x_{B_i} and y_{B_i} too) the actuator displacements for each leg (*i.e.*, a_i and L_i) can take ∞ values which guarantee equations (14) are satisfied.

This fact is typical of kinematically redundant manipulators and will allow to select an appropriate actuation strategy for improving the quality of the moving platform motion. The choice of solution may depend on many criteria (*e.g.*, [1, 5, 12, 13, 14]).

5 JACOBIAN MATRICES AND SINGULARITIES

Equations (4) can be differentiated with respect to time. In matrix form the calculation leads to:

$$
\mathbf{J_z}\dot{\mathbf{z}} = \mathbf{J_q}\dot{\mathbf{q}} \tag{15}
$$

where

$$
\begin{aligned}
\dot{\mathbf{z}} &= \begin{bmatrix} \dot{x} & \dot{y} & \dot{\phi} \end{bmatrix}^T \\
\dot{\mathbf{q}} &= \begin{bmatrix} \dot{a}_1 & \dot{L}_1 & \dot{a}_2 & \dot{L}_2 & \dot{a}_3 & \dot{L}_3 \end{bmatrix}^T
\end{aligned} \tag{16}
$$

and matrices $\mathbf{J_q}$ and $\mathbf{J_z}$ correspond to the manipulator's inverse and forward Jacobian matrices, respectively. The elements of the forward Jacobian matrix $\mathbf{J_z}$ are

$$
\begin{aligned}
J_{z_{1,1}} &= x - h_1 s_\phi; \\
J_{z_{1,2}} &= y + h_1 c_\phi - a_1; \\
J_{z_{1,3}} &= -h_1 c_\phi x - h_1 s_\phi y + h_1 s_\phi a_1; \\
J_{z_{2,1}} &= x - p a_2 + p h_2 c_\phi - q h_2 s_\phi; \\
J_{z_{2,2}} &= y - q a_2 + p h_2 s_\phi + q h_2 c_\phi; \\
J_{z_{2,3}} &= p h_2 c_\phi y - q h_2 s_\phi y - p h_2 s_\phi x - q h_2 c_\phi x + h_2 s_\phi a_2; \\
J_{z_{3,1}} &= x + p a_3 - p h_3 c_\phi - q h_3 s_\phi; \\
J_{z_{3,2}} &= y - q a_3 - p h_3 s_\phi + q h_3 c_\phi; \\
J_{z_{3,3}} &= p h_3 s_\phi x - q h_3 c_\phi x - p h_3 c_\phi y - q h_3 s_\phi y + h_3 s_\phi a_3;
\end{aligned}
$$

whereas the inverse Jacobian matrix $\mathbf{J_q}$ is defined as

$$
\mathbf{J_q} = \begin{bmatrix} h_1 c_\phi + y - a_1 & L_1 & 0 & 0 & 0 & 0 \\ 0 & 0 & h_2 c_\phi + px + qy - a_2 & L_2 & 0 & 0 \\ 0 & 0 & 0 & 0 & h_3 c_\phi - px + qy - a_3 & L_3 \end{bmatrix} \tag{17}
$$

5.1 Inverse singularities

In the kinematically redundant manipulators, inverse singularities (a.k.a. Type 1 singularities) occur when the rank of inverse Jacobian matrix $\mathbf{J_q}$ becomes smaller than the DOF of the moving platform. In other words the singularity occurs when $\det(\mathbf{J_q}\mathbf{J_q}^T) = 0$ [1].

Considering that:

$$
\mathbf{J_q}\mathbf{J_q}^T = \begin{bmatrix} j_1 & 0 & 0 \\ 0 & j_2 & 0 \\ 0 & 0 & j_3 \end{bmatrix} \tag{18}
$$

with

$$
\begin{aligned}
j_1 &= (h_1 c\phi + y - a_1)^2 + L_1^2 = (y_{B_1} - a_1)^2 + L_1^2 \\
j_2 &= (h_2 c\phi + p \cdot x + q \cdot y - a_2)^2 + L_2^2 = (x_{B_2} p + y_{B_2} q - a_2)^2 + L_2^2 \\
j_3 &= (h_3 c\phi - p \cdot x + q \cdot y - a_3)^2 + L_3^2 = (-x_{B_3} p + y_{B_3} q - a_3)^2 + L_3^2
\end{aligned}
$$

Defining $K_1 = y_{B_1} - a_1$, $K_2 = x_{B_2} p + y_{B_2} q - a_2$ and $K_3 = -x_{B_3} p + y_{B_3} q - a_3$, the singularity condition $\det(\mathbf{J_q}\mathbf{J_q}^T) = 0$ can be written as:

$$
\det\left(\mathbf{J_q}\mathbf{J_q}^T\right) = \left(K_1^2 + L_1^2\right)\left(K_2^2 + L_2^2\right)\left(K_3^2 + L_3^2\right) = 0 \tag{19}
$$

It may be noted that equation (19) is satisfied if any one or more diagonal elements are null. Thus, the condition may be expressed as

$$
\begin{aligned}
(y_{B_1} - a_1)^2 + L_1^2 &= 0 \text{ only if } y_{B_1} = a_1 \text{ and } L_1 = 0 \\
(x_{B_2} p + y_{B_2} q - a_2)^2 + L_2^2 &= 0 \text{ only if } x_{B_2} p + y_{B_2} q = a_2 \text{ and } L_2 = 0 \\
(-x_{B_3} p + y_{B_3} q - a_3)^2 + L_3^2 &= 0 \text{ only if } -x_{B_3} p + y_{B_3} q = a_3 \text{ and } L_3 = 0
\end{aligned} \tag{20}
$$

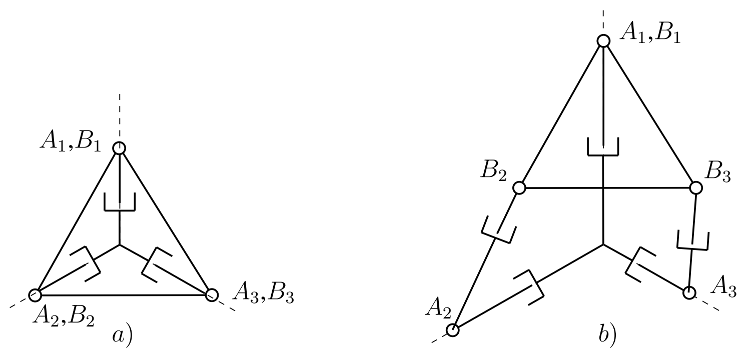

Figure 4: Inverse singularity when a) all branches are in a singular configuration, *i.e.*, $K_i^2 + L_i^2 = 0$ with $i = 1, 2, 3$ and b) branch 1 is in a singular configuration, *i.e.*, $K_1^2 + L_1^2 = 0$.

Figure 4a shows the singularity condition when all diagonal elements in equation (18) are equal to zero whereas Figure 4b shows the pose whenever only branch 1 is in a singular configuration, *i.e.* $K_1^2 + L_1^2 = 0$, where both prismatic joints on leg 1 are parallel. Note that, although not necessary, ϕ has been arbitrarily set to 0 in both figures.

If at least two diagonal terms are zero (Figure 4a) the moving platform looses all its DOF since at least two B_i are fixed. If one (Figure 4b) diagonal term is zero the moving platform preserves only one DOF.

5.2 Direct singularity (Type 2)

The forward Jacobian matrix $\mathbf{J_z}$ in equation (15) can also be expressed as:

$$\mathbf{J_z} = \begin{bmatrix} x_{B_1} & y_{B_1} - a_1 & h_1 \left[a_1 s_\phi - (x_{B_1} c_\phi + y_{B_1} s_\phi)\right] \\ x_{B_2} - pa_2 & y_{B_2} - qa_2 & h_2 \left[a_2 s_\phi - (x_{B_2} c_\delta + y_{B_2} s_\delta)\right] \\ x_{B_3} + pa_3 & y_{B_3} - qa_3 & h_3 \left[a_3 s_\phi - (x_{B_3} c_\lambda + y_{B_3} s_\lambda)\right] \end{bmatrix} \quad (21)$$

where $\delta = \phi + 2\pi/3$ and $\lambda = \phi - 2\pi/3$.

One condition for $\mathbf{J_z}$ to be singular is if all the element in any given row or column are null. Consider, at first, the rows of $\mathbf{J_z}$. Thus, $\mathbf{J_z}$ would be singular whenever:

$$\begin{aligned} x_{B_1} &= 0,\ y_{B_1} = a_1 \text{ for any } \phi \\ x_{B_2} &= pa_2,\ y_{B_2} = qa_2 \text{ for any } \phi \\ x_{B_3} &= -pa_3,\ y_{B_3} = qa_3 \text{ for any } \phi \end{aligned} \quad (22)$$

It should be noted that equations (22) provide the same manipulator poses obtained by equations (20). For that reason they cannot be considered neither Type 1 or Type 2 singularities [15].

Now, consider whenever the columns of $\mathbf{J_z}$ are null.

$$x_{B_1} = 0,\ x_{B_2} = pa_2; x_{B_3} = pa_3 \quad (23)$$

This condition means that links A_iB_i are all parallel to each other (Figure 5a). On the other hand,

$$y_{B_1} = a_1,\ y_{B_2} = qa_2 \text{ and } y_{B_3} = qa_3 \quad (24)$$

means that the manipulator is in the pose shown in Figure 4a.

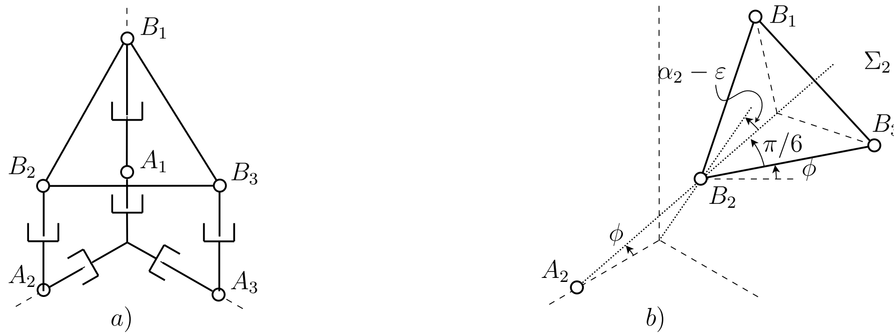

Figure 5: Direct singularity when a) $J_{z_{i,1}} = 0$ and b) $J_{z_{i,3}} = 0$.

Finally,

$$x_{B_1}c_\phi + y_{B_1}s_\phi = a_1 s_\phi, \;\; x_{B_2}c_\delta + y_{B_2}s_\delta = a_2 s_\phi, \text{ and } x_{B_3}c_\lambda + y_{B_3}s_\lambda = a_3 s_\phi \tag{25}$$

represent the condition where links A_iB_i intersect in the moving platform's centroid. Figure 5b illustrates the geometrical interpretation of equations (25). For instance, consider equation (25) for leg 2, where the singularity condition can be re-written as:

$$b_2 \sin(\alpha_2 - \varepsilon) = a_2 s_\phi \tag{26}$$

where $x_{B_2} = b_2 c_{\alpha_2}$, $y_{B_2} = b_2 s_{\alpha_2}$ and $\varepsilon = \phi + \pi/6$. This condition is satisfied if and only if line Σ_2 (Figure 5) passes trough the centroid of the equilateral triangle formed by the moving platform[4]. Similarly it can be shown that the same physical condition applied for legs 1 and 3.

Direct singularities also occur whenever there is linear dependency between rows/columns. More specifically:

- Linear dependency between columns 1 and 2 occurs when A_iB_i ($i = 1, 2, 3$) are parallel.
- Linear dependency between columns 1 and 3 or 2 and 3 occurs when A_iB_i for $i = 1, 2, 3$ all intersect at a common point.
- Linear dependency between rows j ($j = 1, 2, 3$), and k ($k = 2, 3, 1$) occurs whenever A_jB_j and A_kB_k coincide with the edge B_jB_k of the end effector platform.

6 CONCLUSION

The analysis of the new 3-PRPR kinematically redundant planar parallel manipulator was presented in this paper. From the analysis it was found that there are at most six solutions for the forward displacement problem. Conversely, due to the three degrees of kinematic redundancy of the manipulator, the inverse displacement problem has ∞^3 solutions since equations (14) represent three circle of radius L_i and the y-coordinate of the centre being dependent on a_i. It was also shows that, for the symmetrical 3-PRPR, the orientational workspace is a circle. The presence of two P pairs for each branch substantially increases the workspace whose radius is directly proportional to the upper limit of the prismatic joints. A thorough inspection of the singularities shows that inverse singularity configurations cannot occur in practice as these configurations require $L_i = 0$ whereas they would normally be different from zero by construction.

[4] Σ_2 is a line in the direction of the leg L_2 and passing through point A_2.

REFERENCES

[1] Merlet, J.-P., Redundant parallel manipulators, Laboratory Robotics and Automation, **8**(1):17-24, 1996.

[2] Wang, J. and Gosselin C.M.,Kinematic analysis and design of kinematically redundant parallel mechanisms, J. of Mechanical Design, **126**(1):109-118, 2004.

[3] Ebrahimi, I., Carretero J.A., and Boudreau, R., 3-PRRR redundant planar parallel manipulator: Inverse displacement, workspace and singularity analyses, Mechanism and Machine Theory, **42**(8):1007-1016, 2007.

[4] Cha, S., Lasky, T. A. and Velinsky, S. A., Kinematically-Redundant Variations of the 3-RRR Mechanism and Local Optimization-Based Singularity Avoidance, Mechanics Based Design of Structures and Machines, **35**(1):15-38, 2007

[5] Ebrahimi, I., Carretero J.A., and Boudreau, R., Kinematic analysis and path planning of a new kinematically redundant planar parallel manipulator, Robotica, **26**(3):405-413, 2008.

[6] Cheng, H., and Yiu, Y., Dynamics and control of redundantly actuated parallel manipulators, IEEE/ASME Transactions on Mechatronics, **8**(4):483-491, 2003.

[7] Nokleby, S.B., Fisher, R., Podhorodeski, R.P. and Firmani, F., Force capabilities of redundantly-actuated parallel manipulators, Mechanism and Machine Theory, **40**(5):578-599, 2005.

[8] Firmani, F. and Podhorodeski, R.P., Force-Unconstrained Poses for Parallel Manipulators with Redundant Actuated Branches, CSME Transactions, **29**(3):343-356, 2005.

[9] Firmani, F., Zibil, A., Nokleby, S.B., and Podhorodeski, R.P., Force-moment capabilities of revolute-joined planar parallel manipulators with additional actuated branches, CSME Transactions, **31**(2):188-219, 2007.

[10] Ebrahimi, I, Carretero, J.A. and Boudreau, R., A family of kinematically redundant planar parallel manipulators, Journal of Mechanical Design, **130**(6):062306, June 2008.

[11] Merlet, J.-P., *Parallel Robots*, Springer, 2006.

[12] Maciejewski A.A. and Klein C.A., Obstacle avoidance for kinematically redundant manipulators in dynamically variant environments, Int. J. of Robot. Research, **3**(3):109-117,1985.

[13] Nakamura Y., Hanafusa H. and Yoshikawa T., Task-priority based redundancy control of robot manipulators, Int. J. of Robot. Research, **6**(2):3-15,1987.

[14] Nakamura, Y., *Advanced robotics: redundancy and optimization*, Addison-Wesley, 1991.

[15] Bonev, I., *Geometric analysis of parallel mechanisms*, Université Laval, Québec, November 2002.